

Image Flow Estimation Using Facet Model and Covariance Propagation

Ming Ye, Robert M. Haralick
Intelligent Systems Laboratory
Department of Electrical Engineering
University of Washington
Seattle, WA, 98195-2500
{ming,haralick}@george.ee.washington.edu

Abstract

We describe a new image flow estimation method which has three key features: (i) we unify gradient-based and matching-based methods by interpreting a set of gradient-based constraint equations from a matching point of view; (ii) we use a cubic facet model to calculate derivatives accurately. The facet model also acts as a prefilter and provides image noise variance estimates; (iii) we analyze the covariance propagation characteristics of the image flow estimator. Based on the covariance matrices, we use an approximate χ^2 criterion to select the non-zero flow estimates. Our algorithm provides good raw image flow estimates, successfully suppressing false alarms and bad estimates while achieving high detection rate.

1 Introduction

Optic flow is the projected 2D velocity arising from a 3D surface point of an object in motion relative to the camera or observer. Image flow is the optic flow that can be estimated. The estimation methods can be roughly divided into three categories: gradient-based, matching-based and frequency/phase-based. Because of their computational simplicity and satisfactory performance, gradient-based methods are the techniques most extensively studied so far.

There are four steps of processing common to all gradient-based methods: (i) prefiltering or smoothing image sequence to enhance signal-to-noise-ratio and to make the sequence appropriate for the rest of the processing; (ii) estimating spatiotemporal derivatives; (iii) organizing derivative information to form constraints for image flow and solving the

constraints; (iv) selecting the image flow estimates based on the error analysis. While a good model in (iii) lays a sound base for estimation, (i), (ii) and (iv) to a great extent affect the efficiency of the entire algorithm.

We interpret the problem of image flow estimation as that of finding the matching points on the intersection line of the isocontour plane with a successive image frame. This results in a set of gradient-based constraint equations. Gradient-based and matching-based methods are unified in our algorithm. Solving the equations yields the raw image flow estimates.

Barron et al made a comprehensive study on the performance of typical image flow techniques [3][4]. We can find from their work that quite a few existing estimators can provide reasonable raw image flow estimates. However their efficiency usually suffers from the following defects. The prefiltering, if any, is an additional work and is performed by tuning parameters. Most methods use the neighborhood difference as the derivative estimate. It is highly sensitive to noise, in part due to the fact that there was no quantitative error analysis done so that the various tuning parameters could be optimized. Selection of the good estimates is usually heuristic.

The image flow estimator we use is based on facet model and covariance propagation. The facet model incorporates prefiltering, derivative calculation and image noise estimation. It produces good derivative estimates. Covariance propagation provides reliable error analysis. Statistically or physically meaningful selection can be achieved by properly using the covariance information. It works consistently well on different image sequences. False alarms and bad estimates are successfully eliminated while a high

detection rate is achieved.

Section 2 explains the image flow constraint equations. Section 3 constructs the cubic facet model. Section 4 analyzes the covariance propagation characteristics of the image flow estimator. In Section 5 we select the good estimates by a χ^2 selection criterion. Some experimental results are shown in Section 6. We summarize the present and future work in Section 7.

2 Image Flow Constraint Equations

To understand how our image flow constraint equations are developed, let us consider a point moving with velocity $V = (u, v)'$ in an image sequence. Let the point take the coordinates $(0, 0, 0)$ in the 3D space of row, column and time. After a time interval t , the point arrives at a location (x, y, t) . We define a neighborhood $N = X \times Y \times T$ centered at point $(0, 0, 0)$, where X, Y and T are odd numbers. When (x, y, t) is small enough N contains the scope of motion of this point. If we can find the matching point (x, y, t) , the image flow vector V is readily available.

We assume: (i) matching points on different frames have the same intensity value, i.e.,

$$I(x, y, t) = I(0, 0, 0); \quad (1)$$

(ii) the underlying 3D intensity value of this neighborhood is described by a continuous function $I(x, y, t)$; (iii) the motion is translational without acceleration.

To find the matching point, we first construct an isocontour plane at the point $(0, 0, 0)$. We denote by I_x, I_y, I_t the partial derivatives of the intensity with respect to x, y and t and evaluated at $(0, 0, 0)$. The isocontour plane at the point is just the plane orthogonal to the gradient vector described by

$$xI_x + yI_y + tI_t = 0.$$

Intersecting this plane with the frame at t and dividing both sides with t produces the line

$$\frac{x}{t}I_x + \frac{y}{t}I_y + I_t = 0.$$

Since $(\frac{x}{t}, \frac{y}{t}) = (u, v)$, the above equation becomes the famous Optic Flow Constraint Equation (OFCE)

$$I_x u + I_y v + I_t = 0. \quad (2)$$

Thus we have interpret the OFCE as the intersection line of the isocontour plane with a successive image frame, which contains the possible match point.

The matching point (x, y, t) is then located as the point on the line satisfying intensity value match (Eq. (1)). The image flow vector V is determined as $(\frac{x}{t}, \frac{y}{t})'$.

The above procedure finds image flow vector V from a matching point of view. The basic constraints are intersection line OFCE (Eq. (2)) and intensity value match (Eq. (1)). Now let us examine why this procedure works.

Expanding both sides of Eq. (1) as Taylor series around $(0, 0, 0)$ and neglecting the third and higher order terms yield

$$I(x, y, t) = I(0, 0, 0) + xI_x + yI_y + tI_t + \frac{x^2}{2}I_{xx} + xyI_{xy} + \frac{y^2}{2}I_{yy} + xtI_{xt} + ytI_{yt} + \frac{t^2}{2}I_{tt} \quad (3)$$

Matching of spatial intensity pattern around the two corresponding points results in

$$\begin{aligned} I_x(x, y, t) &= I_x(0, 0, 0) = I_x \\ I_y(x, y, t) &= I_y(0, 0, 0) = I_y \end{aligned}$$

Since motion is uniform with no acceleration, the temporal derivative of the intensity must match. This yields

$$I_t(x, y, t) = I_t(0, 0, 0) = I_t$$

Applying these constraints to Eq. (3) we have

$$xI_x + yI_y + tI_t + \frac{x^2}{2}I_{xx} + xyI_{xy} + \frac{y^2}{2}I_{yy} + xtI_{xt} + ytI_{yt} + \frac{t^2}{2}I_{tt} = 0 \quad (4)$$

$$xI_{xx} + yI_{xy} + tI_{xt} = 0 \quad (5)$$

$$xI_{yx} + yI_{yy} + tI_{yt} = 0 \quad (6)$$

$$xI_{tx} + yI_{ty} + tI_{tt} = 0 \quad (7)$$

Multiplying Eq. (5), (6) and (7) by x, y, t respectively and adding them together yields

$$x^2I_{xx} + 2xyI_{xy} + y^2I_{yy} + 2xtI_{xt} + 2ytI_{yt} + t^2I_{tt} = 0.$$

Substituting the above equation back into Eq. (4) yields

$$xI_x + yI_y + tI_t = 0,$$

the OFCE. Thus, the technique of using Eq. (2) and Eq. (1) in essence works because it assumes that all first partials are matching. Therefore to calculate V , we just need to find $V = (u, v)'$ to minimize

$$\|AV - b\|^2 \quad (8)$$

where

$$A = \begin{pmatrix} I_x & I_y \\ I_{xx} & I_{xy} \\ I_{yx} & I_{yy} \\ I_{tx} & I_{ty} \end{pmatrix} \quad b = - \begin{pmatrix} I_t \\ I_{xt} \\ I_{yt} \\ I_{tt} \end{pmatrix}.$$

This is a typical gradient-based constraint system. We begin with finding matching points, and finish by gradient-based constraints. Matching and gradient-based methods are unified in our algorithm.

Once A and b are available, the group of equations can be solved for (u, v) by standard least-square methods. This approach was first described in [1].

3 Facet Model

The facet model is used to estimate the derivatives required in Eq.(8). The facet model principle states that the image can be thought of as a piecewise continuous gray level intensity surface perturbed by certain noise. With the noise-free model and the noise model defined, all processings can be applied to the noise-free model, and the impact of the noise can be examined quantitatively.

3.1 Cubic Facet Model

A noise-free cubic model is defined as

$$I(x, y, t) = a_1 + a_2x + a_3y + a_4t + a_5x^2 + a_6xy + a_7y^2 + a_8yt + a_9t^2 + a_{10}xt + a_{11}x^3 + a_{12}x^2y + a_{13}xy^2 + a_{14}y^3 + a_{15}y^2t + a_{16}yt^2 + a_{17}t^3 + a_{18}x^2t + a_{19}xt^2 + a_{20}xyt, \quad x, y, t \in N. \quad (9)$$

We assume the independent and additive noise with zero mean and variance σ^2 . Thus the 3D neighborhood is completely characterized by the facet parameters a_k 's and noise variance σ^2 .

σ^2 is generally unknown. We assume it is a constant in each neighborhood. A least-square fitting can be used to estimate a_k 's and σ^2 by finding the coefficient vector a to minimize

$$\|Da - J\|^2 \quad (10)$$

where

$$D = \begin{pmatrix} 1 & x_1 & y_1 & t_1 & \dots & x_1y_1t_1 \\ 1 & x_1 & y_1 & t_2 & \dots & x_1y_1t_2 \\ \vdots & \vdots & \vdots & \vdots & & \vdots \\ 1 & x_1 & y_2 & t_2 & \dots & x_1y_2t_1 \\ \vdots & \vdots & \vdots & \vdots & & \vdots \\ 1 & x_X & y_Y & t_T & \dots & x_Xy_Yt_T \end{pmatrix} \quad J = \begin{pmatrix} J_1 \\ J_2 \\ \vdots \\ J_N \end{pmatrix}$$

J_n is the image intensity at (x_i, y_j, t_k) . σ^2 is estimated by

$$\hat{\sigma}^2 = \frac{1}{N-20} \|Da - J\|^2$$

The covariance matrix of the twenty facet parameters is available as a by-product of the least-square procedure.

We do not solve the least-square problem of Eq.(10) in the brute-force manner. Rather we define the discrete orthogonal cubic basis functions of x, y and t , efficiently solve for the coefficients of the discrete orthogonal basis functions using the separability properties and then determine the coefficient vector a as the appropriate linear combinations [5].

3.2 Derivative Calculation and the OFCEs

All the derivatives are merely scaled facet parameters. We substitute these derivatives into the image flow constraint equations Eq. (8) obtaining the actual OFCEs with A and b defined as

$$A = \begin{pmatrix} a_2 & a_3 \\ 2a_5 & a_6 \\ a_6 & 2a_7 \\ a_{10} & a_8 \end{pmatrix} \quad b = - \begin{pmatrix} a_4 \\ a_{10} \\ a_8 \\ 2a_9 \end{pmatrix} \quad (11)$$

3.3 Advantages of Facet Model in Image Flow Estimation

Derivative calculation is the lowest-level element of gradient-based image flow estimators. It greatly affects the efficiency of the entire algorithm.

Many image flow estimation algorithms calculate the neighborhood difference as derivative estimates. Such an approach is highly sensitive to noise. An additional prefilter or smoother is needed before derivative estimation. This requires extra work independent of the image flow estimation. Barron [3] suggested a spatiotemporal Gaussian prefilter. It assumes a uni-variance Gaussian noise model in the entire sequence. The variance σ^2 of this prefilter needs hand-tuning according to different image sequences. Fifteen frames are required for $\sigma = 1.5$. When the number of frames available is limited, this method will be a problem.

In our facet model, we first reconstruct the underlying smooth function from noisy image data by facet fitting, and then we perform all operations upon the smooth fitting function. This smooth function can be looked on as a prefiltered version of the noisy image sequence. We do not need an extra prefilter. The facet model allows different noise variance in each neighborhood. This is more appropriate than the uni-variance model. For any fixed neighborhood size, the derivatives estimated by the facet model tend to have smaller variances than the estimates derived from differences and prefiltering.

4 Error Analysis Through Covariance Propagation

The image flow estimation suffers from several major sources of errors. (i) Error from violations of the assumptions. For example, we assume the intensity of the image sequence neighborhood is smooth enough to be fitted to a cubic facet model, while large jumps of intensity especially at object boundaries often are not well fit by a cubic polynomial. Image flow estimates at places of occlusion, transparency and high texture are extremely unreliable. This is a problem with all the existing image flow estimation methods. (ii) Error from error propagation characteristics. If the matrix A is ill-conditioned, the system will become too sensitive to input error to be stable. (iii) Error from image data, such as quantization error, measurement error, small brightness change. All sources of error finally propagate to the image flow estimate.

With the existence of so much noise, the error analysis on the image flow estimates becomes a crucial issue. Measuring confidence of estimation, selecting the good estimates and evaluating the robustness of the algorithms should all inherently be based on the error analysis. Unfortunately, such work is not widely carried out.

The lack of error analysis makes many of the existing image flow estimators not applicable in regions with severe noise. Some methods provide confidence measurement on image flow estimates and select good estimates based on them. These measurements, such as singular value ratio, condition number, do not have an explicit relationship with the estimation error, so selection based on them are not reliable. We can observe from the literature, after these selections, quite a few false alarms and bad estimates are still there, while some good estimates are removed. Furthermore, we do not know how to determine the appropriate selection criteria, say, a threshold. Even if an appropriate threshold is achieved, we still do not know the theoretical reason that we choose this value instead of others. When the input is changed, the value has to be adjusted and trials have to be repeated.

Much effort has been made to find a confidence measure to evaluate the goodness of image flow estimators. For synthetic image sequences, some error measurements can be defined with the knowledge of the ground truth. However no agreement has been reached on an appropriate measurement. When we go to real images, things get even worse. People only look at the results and evaluate them by the eye.

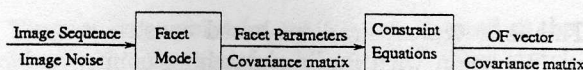


Figure 1: System block diagram of our algorithm

We introduced covariance propagation analysis [2] to solve these problems in a systematic way. We propagate all sources of errors to image flow vectors, obtaining a covariance matrix as the error measurement with each image flow estimate, and then a selection scheme based on the covariance matrix is used to reject the unreliable estimates. The selection has a clear statistical meaning and is therefore widely applicable.

4.1 Covariance Propagation Characteristic Analysis

The goal of covariance propagation is to propagate the input error step by step through a system to obtain the perturbation on the output.

Our image flow estimation algorithm consists of two steps: first fitting the image sequence neighborhood to a facet model, second estimating the image flow vector (u, v) at the central pixel $(0, 0, 0)$ of the neighborhood. The covariance propagation also has two steps: first propagating the image noise to the facet parameters, second finding the covariance matrix of the image flow vector from that of the facet parameters. The procedure is shown in Fig. 1.

The following assumptions are made in covariance propagation: (i) the noise is independent and additive with zero mean and variance σ^2 ; (ii) the system is approximately linear for small perturbation σ . If the noise is not independent and has a known correlation matrix, then the covariance propagation technique can easily be generalized to accommodate colored noise.

In the facet model fitting step, we calculate the facet parameters $\hat{a} = (a_1, a_2, \dots, a_{20})$ and the covariance matrix $\hat{\Sigma}_{\hat{a}}$ associated with them. We use the hat sign '^' to indicate the estimate of the true value.

We use the facet parameters $\hat{X} = (a_2, a_3, \dots, a_{10})$ in the image flow estimation step. We consider the image flow estimator as a system with input \hat{X} , which are random variables with covariance matrix $\hat{\Sigma}_{\hat{X}}$, a 9×9 submatrix of $\hat{\Sigma}_{\hat{a}}$, and with the output image flow vector $\hat{V} = (\hat{u}, \hat{v})$, with its covariance matrix $\hat{\Sigma}_{\hat{V}}$.

$F(X, V)$, the criterion function we use to estimate V , is defined by:

$$F(X, V) = (AV - b)'(AV - b) \quad (12)$$

where A, V, b are defined in Eq. (11).

We take partial derivatives of $F(X, V)$ with respect to V forming the gradient vector $g(X, V)$ of F . The gradient g is a 2×1 function.

The second order partial derivatives of F with respect to V is

$$\frac{\partial g(X, V)}{\partial V} = 2 \begin{pmatrix} p_1 & p_2 \\ p_2 & p_3 \end{pmatrix} \quad (13)$$

where

$$\begin{aligned} p_1 &= a_2^2 + 4a_5^2 + a_6^2 + a_{10}^2 \\ p_2 &= a_2a_3 + 2a_5a_6 + 2a_6a_7 + a_8 \\ p_3 &= a_3^2 + a_6^2 + 4a_7^2 + a_8^2. \end{aligned}$$

The second order partial derivatives with respect to X is

$$\frac{\partial g(X, V)}{\partial X} = 2 \times \begin{pmatrix} 2a_2u + a_3v + a_4 & a_3u \\ a_2v & a_2u + 2a_3v + a_4 \\ a_2 & a_3 \\ 8a_5u + 2a_6v + 2a_{10} & 2a_6u \\ 2v(a_5 + a_7) + 2a_6u + a_8 & 2u(a_5 + a_7) + 2a_6v + a_{10} \\ 2a_6v & 2a_6u + 8a_7v + 2a_8 \\ a_6 + a_{10}v & 2a_7 + a_{10}u + 2a_8v + 2a_9 \\ 2a_{10} & 2a_8 \\ 2a_5 + 2a_{10}u + a_8v + 2a_9 & a_6 + a_8u \end{pmatrix} \quad (14)$$

The solution $\hat{V} = V + \Delta V$ must be a zero of $g(\hat{X}, \hat{V})$. Now taking a Taylor series expansion of g around (X, V) we obtain to a first order approximation:

$$g(X + \Delta X, V + \Delta V) = g(X, V) + \frac{\partial g'}{\partial X}(X, V)\Delta X + \frac{\partial g'}{\partial V}(X, V)\Delta V.$$

But since $V + \Delta V$ extremizes $F(X + \Delta X, V + \Delta V)$, $g(X + \Delta X, V + \Delta V) = 0$. Also, since V extremizes $F(X, V)$, $g(X, V) = 0$. Thus to a first order approximation,

$$0 = \frac{\partial g'}{\partial X}(X, V)\Delta X + \frac{\partial g'}{\partial V}(X, V)\Delta V$$

Since the relative extremum of F is a relative minimum, the matrix

$$\frac{\partial g}{\partial V}(X, V) = \frac{\partial F^2}{\partial^2 V}(X, V)$$

must be positive definite for all (X, V) . This implies that $\frac{\partial g}{\partial V}(X, V)$ is non-singular. Hence $(\frac{\partial g}{\partial V})^{-1}$ exists and since it is symmetric we can write:

$$\Delta V = -(\frac{\partial g}{\partial V}(\hat{X}, \hat{V}))^{-1} \frac{\partial g'}{\partial X}(\hat{X}, \hat{V})\Delta X$$

which relates how the random perturbation ΔX on X propagates to the random perturbation ΔV on V . If the expected value of ΔX , $E[\Delta X]$, is zero, then from this relation we see the $E[\Delta V]$ will also be zero, to a first order approximation.

This relation also permits us to calculate the covariance of the random perturbation ΔV .

$$\begin{aligned} \Sigma_{\Delta V} &= E[\Delta V \Delta V'] \\ &= (\frac{\partial g}{\partial V})^{-1} \frac{\partial g'}{\partial X} \Sigma_{\Delta X} \frac{\partial g}{\partial X} (\frac{\partial g}{\partial V})^{-1} \end{aligned}$$

Thus to the extent that the first order approximation is good, (i.e. $E[\Delta V] = 0$), then

$$\Sigma_{\hat{V}} = \Sigma_{\Delta V}$$

The way in which we have derived the covariance matrix for ΔV based on the covariance matrix for ΔX requires that the matrices

$$\frac{\partial g}{\partial V}(X, V) \text{ and } \frac{\partial g}{\partial X}(X, V)$$

be known. But the true values X and V are not observed. Only $X + \Delta X$ and $V + \Delta V$ are available. So if we want to determine an estimate $\hat{\Sigma}_{\hat{V}}$ for the covariance matrix $\Sigma_{\hat{V}}$, we can proceed by expanding $g(X, V)$ around $g(X + \Delta X, V + \Delta V)$.

$$\begin{aligned} g(X, V) &= g(X + \Delta X, V + \Delta V) \\ &\quad - \frac{\partial g'}{\partial X}(X + \Delta X, V + \Delta V)\Delta X \\ &\quad - \frac{\partial g'}{\partial V}(X + \Delta X, V + \Delta V)\Delta V \end{aligned}$$

Here we find in a similar manner,

$$\begin{aligned} \Delta V &= -(\frac{\partial g}{\partial V}(X + \Delta X, V + \Delta V))^{-1} \\ &\quad \frac{\partial g'}{\partial X}(X + \Delta X, V + \Delta V)\Delta X \end{aligned}$$

This motivates the estimator $\hat{\Sigma}_{\Delta V}$ for $\Sigma_{\Delta V}$ defined by

$$\begin{aligned} \hat{\Sigma}_{\Delta V} &= (\frac{\partial g}{\partial V}(\hat{X}, \hat{V}))^{-1} \frac{\partial g'}{\partial X}(\hat{X}, \hat{V})\Sigma_{\Delta X} \\ &\quad \frac{\partial g}{\partial X}(\hat{X}, \hat{V})(\frac{\partial g}{\partial V}(\hat{X}, \hat{V}))^{-1} \end{aligned}$$

So to the extent that the first order approximation is good, $\hat{\Sigma}_{\hat{V}} = \hat{\Sigma}_{\Delta V}$.

Since

$$\frac{\partial g}{\partial V}(\hat{X}, \hat{V}) \text{ and } \frac{\partial g}{\partial X}(\hat{X}, \hat{V})$$

can be calculated from Eq. (13) and (14) by substituting into the estimates of facet parameters \hat{X} and image flow vector \hat{V} , till now we have accomplished the covariance propagation analysis.

4.2 Error Analysis Based on Covariance Matrix

When the assumption of small image noise holds, the covariance propagation yields a covariance matrix with each image flow vector, indicating the estimation error.

However as we have discussed in Section 4, the error on estimates come from more complicated sources than the assumed small image noise. High texture regions, homogeneous regions, and regions with abrupt intensity variation, create great difficulties for image flow estimators. These errors exceed the linear range of the system, thus the first order approximation is no longer valid. Can we still use the covariance propagation results as the confidence measure? This answer is yes. High texture or homogeneous regions make the matrix D in Eq. (10) or A in Eq. (11) near singular. This produces huge variances associated with image flow estimates. Regions with abrupt intensity variation cause large facet fitting error, which when propagated to the image flow estimates, also produces large variances. Since these outliers exhibit themselves with abnormally large variances of image flow estimates, the covariance matrix is still a consistent and reliable measurement of the error on image flow estimates.

5 Selection

Image flow estimators usually provide 100% dense flow fields. Within these estimates, there are misdetections in homogeneous regions, false alarms due to image noise or slight brightness change, and bad estimates due to texture or occlusion. The goal of postprocessing the raw estimates is to eliminate the false alarms and the bad estimates as much as possible, while preserving the lowest misdetection rate. To achieve this, we use a χ^2 selector.

We assume the velocities u and v are statistically independent. Therefore the estimated variances σ_u^2, σ_v^2 describe the noise on u and v . Under the hypothesis of zero velocity, $u = 0, v = 0$, the statistic χ^2 defined by

$$\chi^2 = \frac{u^2 + v^2}{\sigma_u^2 + \sigma_v^2}.$$

has an approximate χ^2 distribution with 2 degrees of freedom. When the χ^2 value is too low, we judge the image flow vector as being insignificantly different from zero. Thus we set the flow vector to 0. When the χ^2 value is high enough we use the calculated (u, v) value as the estimated image flow vector.

We set a threshold on the χ^2 values and reject the hypothesis of $u = v = 0$ when χ^2 is larger than the threshold. After the selection, the remaining image flow vectors are good estimates of the true values.

6 Experiments

Our experiments use a neighborhood size of $5 \times 5 \times 5$ to estimate the facet parameters.

In the 'Hamburg Taxi Sequence' [3] (Fig. 2(a)) there are four moving objects: (i) the taxi turning the corner; (ii) a car in the lower left, driving from the left to the right; (iii) a van in the lower right driving right to left; and (iv) a pedestrian in the upper left walking across the street from the right to the left. Image speeds of the four moving objects are approximately 1.0, 3.0, 3.0 and 0.3 pixels/frame respectively. The background scene is still.

In [3], Barron provided the flow field plots for the 'TAXI' sequence of nine typical image flow techniques. Most of these estimators give reasonable raw estimates. However, four of them leave the flow field unselected; and the selections by the rest five techniques are not quite successful. After their selections, the image flow vectors of the car or the van, or both of them are gone, while a lot of false alarms are still there. None of them singled out the motion of the pedestrian.

Fig. 2(b) shows the unselected image flow estimates of our algorithm. For the sake of clarity, we sampled the flow field by 2×2 . We can see the correct motion trend and the shapes of the objects. There are many false alarms; the motion of the pedestrian is inundated in the false alarms; and there are also some bad estimates, such as the vectors with fairly big magnitude pointing to the left on the taxi.

Then we conducted the selection. The effect is apparent (Fig. 2(c), sampled by 2×2). Nearly all the false alarms and bad estimates are removed. We can clearly observe the four moving objects: the taxi, the car, the van and the pedestrian. Their relative velocities conform to the a prior knowledge. The motion of the pedestrian, which was indiscernible from the background false alarms, now is clearly singled out. Compared with the results given in [3], our method produces the best performance for this sequence.

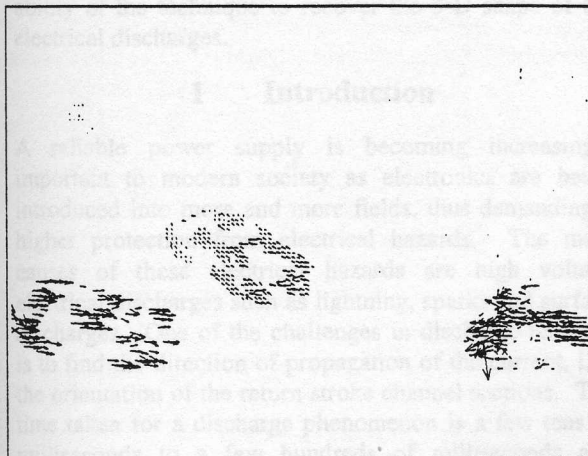
We processed other image sequences with our algorithm, the results are similar with that of the TAXI sequence. Especially, the same threshold produced consistently good performance. This means our selection is scene-insensitive.



(a) TAXI sequence: the frame image flow is computed on



(b) Image flow estimates without thresholding



(c) After χ^2 selection

The χ^2 selection is consistently good because it has a clear statistical meaning. We only use the image flow vector estimates that are statistically different from zero.

7 Summary

The contribution of our image flow estimation algorithm lies in three aspects.

First, gradient-base and matching-base methods are unified by interpreting a set of gradient-based constraint equations from a matching point of view. The resulted OFCEs provide good raw image flow estimates.

Secondly, the derivatives are accurately calculated with a cubic facet model. The facet model also acts as a prefilter and provides image noise variance estimate.

Finally, the error analysis is carried out by covariance propagation. Based on the covariance matrix, a χ^2 selection is defined to select the good estimates. This selection scheme successfully suppresses the false alarms and bad estimates while achieving high detection rate.

The preliminary work has shown satisfactory results. More research is being carried out on quantitative performance evaluation, improving the selection and comparing with other algorithms through extensive experiments.

References

- [1] Robert M. Haralick, Jong S. Lee. The facet approach to optic flow. Proceedings of the Image Understanding Workshop, VA, 1983.
- [2] Robert M. Haralick. Propagating Covariance In Computer Vision. International Journal of Pattern Recognition and Artificial Intelligence, vol.10, no.5. pp. 561-72. Aug. 1996.
- [3] J.L. Barron, et al. Performance of Optical Flow Techniques. International Journal of Computer Vision, 12:1, 43-77, 1994.
- [4] J.L. Barron, et al. On Optical Flow. Proceedings of the Sixth International Conference on Artificial Intelligence and Information-Control Systems of Robots, Smolenice Castle, Slovakia, Sep 12-16, 1994.
- [5] Robert M. Haralick, et al. Computer and Robot Vision. Addison-Wesley publishing company, 1992, Chapter 8, Vol. 1; Chapter 15, Vol. 2.

Figure 2: Experiment results of TAXI sequence

- [6] Berthold K.P. Horn and Brian G. Schunck. Determining Optic Flow. *Artificial Intelligence*, vol. 17, pp. 185-203, 1981.
- [7] H.H. Nagel. On the estimation of optical flow: relations between different approaches and some new results, *Artificial Intelligence*, vol.33, pp.299-324, 1984.
- [8] J.K. Kearney, et al. Optical flow estimation: an error analysis of gradient-based methods with local optimization, *IEEE Transactions on Pattern Analysis and Machine Intelligence*, vol. PAMI-9, No.2, March 1987.
- [9] William H. Press, et al. *Numerical Recipes in C*, 2nd Edition. Cambridge University Press, 1994.
- [10] Jongsoo Lee. FACET3. GIPSY, Intelligent Systems laboratory, 1983.

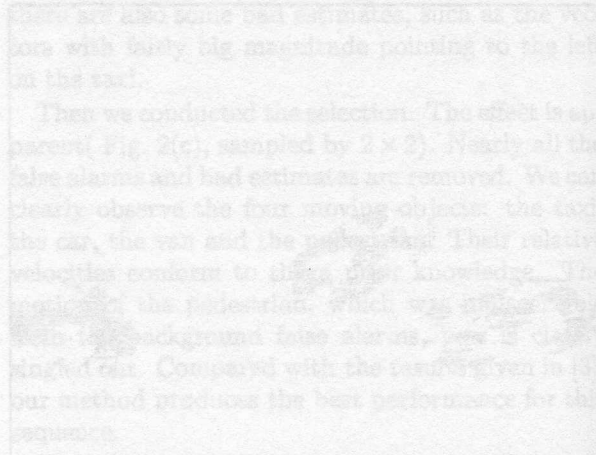
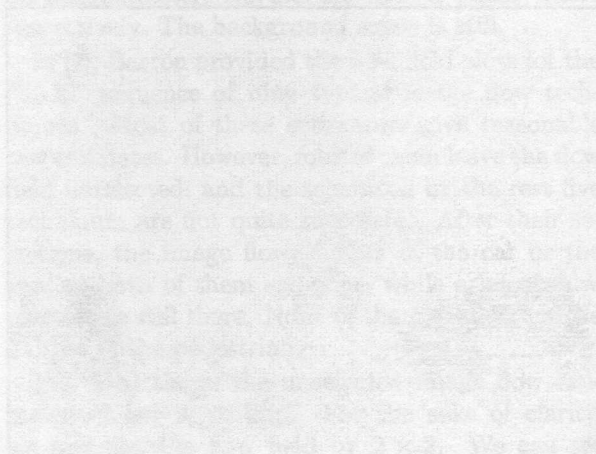
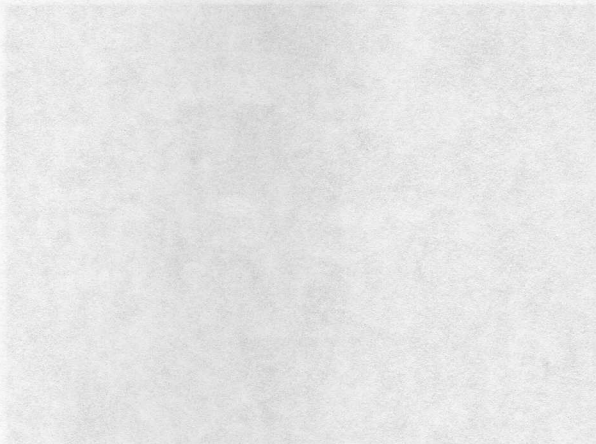


Figure 2. Experimental results of FACET3. (a) Original image, (b) image after optical flow estimation, (c) image after optical flow estimation with local optimization.